LANGMUIR

pubs.acs.org/Langmuir Article

Balancing Enzyme Encapsulation Efficiency and Stability in Complex Coacervate Core Micelles

Riahna Kembaren, Remco Fokkink, Adrie H. Westphal, Marleen Kamperman, J. Mieke Kleijn, and Jan Willem Borst*

Cite This: *Langmuir* 2020, 36, 8494–8502

Read Online

ACCESS | Metrics & More | Article Recommendations | Supporting Information

ABSTRACT: Encapsulation of charged proteins into complex coacervate core micelles (C3Ms) can be accomplished by mixing them with oppositely charged diblock copolymers. However, these micelles tend to disintegrate at high ionic strength. Previous research showed that the addition of a homopolymer with the same charge sign as the protein improved the stability of protein-containing C3Ms. In this research, we used fluorescence correlation spectroscopy (FCS) and dynamic light scattering (DLS) to study how the addition of the homopolymer affects the encapsulation efficiency and salt stability of the micelles. We studied the encapsulation of laccase spore coat protein A (CotA), a multicopper oxidase, using a strong cationic-neutral diblock copolymer, poly(*N*-methyl-2-vinyl-pyridinium iodide)-*block*-poly(ethylene oxide) ($PM2VP_{128}$-*b*-PEO_{477}), and a negatively charged homopolymer, poly(4-styrenesulfonate) (PSS_{215}). DLS indeed showed an improved stability of this three-component C3M system against the addition of salt compared to a two-component system. Remarkably, FCS showed that the release of CotA from a three-component C3M system occurred at a lower salt concentration and over a narrower concentration range than the dissociation of C3Ms. In conclusion, although the addition of the homopolymer to the system leads to micelles with a higher salt stability, CotA is excluded from the C3Ms already at lower ionic strengths because the homopolymer acts as a competitor of the enzyme for encapsulation.

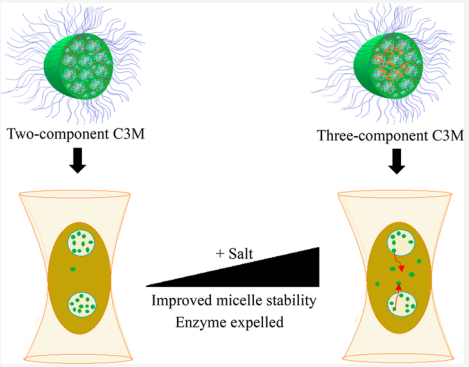

INTRODUCTION

Complex coacervate core micelles (C3Ms) can be formed by mixing a diblock copolymer composed of a neutral block and a charged block with an oppositely charged polyelectrolyte or a charged biomolecule, such as DNA,[1] RNA,[2] or protein.[3,4,45] The oppositely charged parts bind electrostatically to form an almost electroneutral coacervate. This coacervate forms the core of the micelle, surrounded by a corona consisting of the neutral hydrophilic parts of the diblock copolymer, which keeps the micelles in solution.[5] C3Ms can be used for a wide variety of applications, for example, as nanoreactors,[6] diffusional nanoprobes,[7] anti-biofouling coatings,[8] and drug delivery systems.[9] Advantages of C3Ms as a packing system for proteins are their solubility in aqueous solution, that many protein molecules can be encapsulated in one micelle,[3] and that they offer opportunities for controlled release.[10] Encapsulation of proteins can protect them against detrimental environmental effects and protease activity, and enzyme-containing C3Ms can be used as a microreactor to overcome incompatibility problems between polar enzymes and nonpolar substrates.[11]

For the encapsulation of a protein in C3Ms, the total protein charge and charge distribution over its surface are very important and are dependent upon the amino acid composition, structure, and pH of the surrounding solution.[4] In addition, because of the hydrophobic nature of various amino acid residues, the formation of protein-containing C3Ms may not only be driven by electrostatic interactions and entropy gain as a result of counterion release[12] but hydrophobic interactions may also contribute significantly.[13]

One of the most significant challenges regarding the use of C3Ms as packing systems for proteins is that they easily disintegrate, often as a result of the low charge density of proteins. Lindhoud et al. showed, using dynamic light scattering (DLS), that the most stable enzyme-containing C3Ms could be obtained by adding a homopolymer with the same charge sign as the protein to the two-component system, in excess over the protein concentration.[14] Research from Black et al. showed that bovine serum albumin (BSA) could be encapsulated in coacervate droplets of two oppositely charged polypeptides. However, increasing the ratio of BSA to the total

Received: April 14, 2020
Revised: June 29, 2020
Published: June 29, 2020

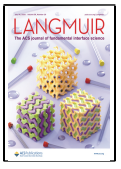

https://dx.doi.org/10.1021/acs.langmuir.0c01073
Langmuir 2020, 36, 8494–8502

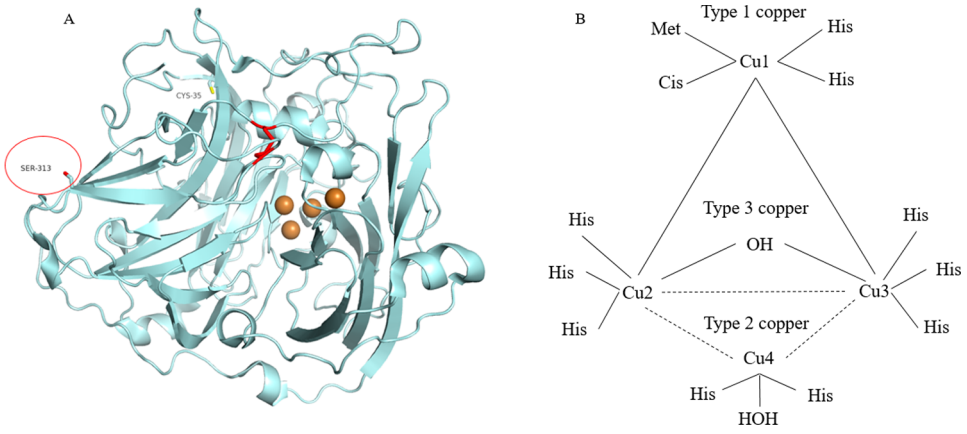

Figure 1. (A) CotA wild-type structure. Cu atoms are represented as spheres colored in brown. The protein contains one disulfide bridge, which is represented as a red line. (B) Copper coordination in the CotA laccase structure.[23,28]

amount of polypeptides in the system led to a less than linear increase of BSA in the coacervate, as observed using a Bradford colorimetric assay.[15] This illustrates the need for further investigation of three-component coacervate systems for protein encapsulation, studied using additional techniques, as already suggested by Blocher and Perry.[16]

In 2010, Gapinski et al. showed that the relatively novel technique of fluorescence correlation spectroscopy (FCS) could be used to measure micellar sizes and shapes.[17] Research of Nolles et al. showed that DLS and FCS provided similar results concerning the hydrodynamic radius and preferred micellar composition (PMC) of two-component C3Ms that contained green fluorescent protein (GFP).[45] In addition, FCS enabled them to obtain the distribution of protein over micelles and solution and the number of protein molecules incorporated per micelle.[3] In comparison to DLS, FCS has a relatively low background noise as a result of the Stokes shift of the fluorescence emission and measurements can be conducted at very low (nanomolar) concentrations. Furthermore, FCS has a selectivity that allows for the measurement of specific fluorescent molecules in systems.[18] On the other hand, FCS experiments and analysis are more labor-intensive than DLS measurements, and often fluorescence labeling of biomolecules is required.

The spore coat protein A (CotA) laccase is the model enzyme of the present study. CotA is originally found in the outer coat layer of the *Bacillus subtilis* endospore.[19] CotA has an isoelectric point (pI) at pH 5.84 and a molar weight of 65 kDa. It is a multicopper oxidase (MCO), characterized by the presence of four copper ions[20] (Figure 1). These four copper ions are classified into three categories based on the ultraviolet/visible (UV/vis) and electronic paramagnetic resonance (EPR) spectra, denoted as type 1 (T1), type 2 (T2), and type 3 (T3).[21] The T1 Cu ion is responsible for the intense blue color of the enzyme, and its absorption can be detected around 600 nm. The T2 and two T3 Cu ions form the trinuclear center (TNC) in the protein structure.[22] CotA can catalyze the oxidation of a wide variety of substrates using dioxygen as an electron acceptor. Substrate oxidation occurs at the T1 binding pocket, and the electrons are then transferred to the TNC, where the reduction of dioxygen occurs.[23,24] CotA has a region of positive charge on its surface at the interface between domains 1, 2, and 3, including 10 lysine and 5 arginine amino acid residues.[25] The biological function of this positively charged patch is its involvement in the assembly of CotA into the spore outer coat layer.[6]

Some types of laccases have already been used as a model to study enzyme immobilization. For example, Pich et al. used laccase from fungus in their study of composite magnetic particles as enzyme carriers,[26] while Bryjak et al. immobilized laccase from fungus by covalently binding it to a copolymer of butyl acrylate and ethylene glycol dimethacrylate.[27] However, thus far, laccases have not been used to study encapsulation in complex coacervate core micelles. In this research, we studied the stability and encapsulation efficiency of CotA containing C3Ms. We show that a combination of DLS and FCS data is necessary to optimize the balance between micelle stability and encapsulation efficiency.

EXPERIMENTAL SECTION

Materials. 2,2′-Azino-bis(3-ethylbenzothiazoline-6-sulfonic acid) (ABTS) was purchased from Sigma-Aldrich. The probe Alexa Fluor C5 maleimide (Alexa488) was purchased from Thermo Fisher Scientific. The diblock copolymer poly(2-vinylpyridinium iodide)$_{128}$-*block*-poly(ethylene oxide)$_{477}$ (M_n = 34.5 kg/mol; M_w/M_n = 1.1) was obtained from Polymer Source, Inc., Canada. This diblock copolymer then was quaternized with iodomethane following the procedure described by Lindhoud et al.[29] The quaternization degree was about 70% as measured by ^{1}H nuclear magnetic resonance (NMR) (see Figure S1 of the Supporting Information).[30] The homopolymer poly(4-styrenesulfonate)$_{215}$ (M_n = 43 kg/mol; M_w/M_n = 1.03; degree of sulfonation of about 90%) was purchased from Polymer Source, Inc., Canada.

CotA Production. The production and purification of CotA were performed following the procedure described by Martins et al.[19] The CotA gene was cloned into a pLOM 10 vector and heterologously expressed in *Escherichia coli* Rosetta cells. The induction of CotA laccase expression was performed by adding 0.1 mM isopropyl β-D-1-thiogalactopyranoside (IPTG) and 0.25 mM $CuSO_4$ at 25 °C. The purification of CotA laccase was performed using cation-exchange chromatography (cIEX using a SP-Sepharose FF column from GE Healthcare) and gel filtration chromatography (Superdex 200 column from GE Healthcare).

A variant of CotA was obtained by replacing a serine at position 313 in the amino acid sequence by a cysteine (CotA S313C). Copper is an oxidation catalyst that can promote the oxidation of free sulfhydryl in cysteine of CotA S313C. Because of that reason, for this variant, apoenzyme was produced, i.e., without the addition of 0.25 mM $CuSO_4$ during induction.[31] The CotA-containing fractions from cIEX were pooled and subsequently labeled with Alexa Fluor 488 C5 maleimide with a molar ratio of 1:10 at 4 °C by incubation in the dark for 16 h. Next, the mixture was loaded to a Biogel-P6DG gel filtration

https://dx.doi.org/10.1021/acs.langmuir.0c01073
Langmuir 2020, 36, 8494−8502

column (BioRad) to separate the labeled protein from the unreacted label. The fractions that showed fluorescence and contained protein were pooled and concentrated using an Amicon concentrator (cutoff of 10 kDa). The pooled concentrated enzyme was then loaded to a gel filtration column (Superdex 200 column). The fractions that showed absorptions at both 280 and 490 nm were collected and concentrated. The purity of labeled CotA was analyzed using sodium dodecyl sulfate polyacrylamide gel electrophoresis (SDS−PAGE) analysis.

pH Stability of CotA: Enzyme Activity Test and Circular Dichroism (CD). For the activity assay (standard assay), we used 1 mM ABTS as a substrate for CotA. The assay was performed in 0.1 M sodium acetate buffer at pH 4.4. The oxidation product, the green-colored cationic radical ($ABTS^{\bullet+}$), was measured spectrophotometrically at 420 nm (ε = 36 000 M^{-1} cm^{-1}). A total of 1 unit of laccase activity was defined as the amount of laccase that oxidized 1 μmol of ABTS per minute at 25 °C.

To determine the stability of CotA at different pH values, the buffer of the enzyme solution was exchanged with buffers of pH 7.6, 9.0, and 10.8 at 4 °C. The enzyme solutions were incubated at the three pH values and room temperature and sampled every 5 min up to a total of 1 h. The samples were assayed using the standard assay. Next to the activity measurements, we also performed CD spectroscopy at the three pH values, after incubation for 1 h, to determine any secondary structure changes of CotA. CD experiments were performed on a JASCO J-715 spectropolarimeter with a Jasco PTC 348 WI temperature controller. The far-UV CD spectra were recorded from 200 to 260 nm at 25 °C. The sample was loaded into a quartz cuvette with an optical path length of 1 mm. A total of 20 spectra, each recorded with a resolution of 1 nm and a scan speed of 50 nm/min, were accumulated and averaged.

Preparation of Protein-Containing C3Ms. Enzyme and polymer solutions containing 10 mM sodium carbonate buffer were prepared, with a final pH of 10.8. All of the solutions were filtered using a 0.2 μm poly(ether sulfone) membrane syringe filter (Advanced Microdevices Pvt. Ltd.). The PMC of the two-component C3Ms was determined by mixing a constant concentration of CotA with different concentrations of PM2PV-*b*-PEO. DLS measurements were performed to determine at which charge composition optimal micelle formation took place.

The amino acid sequence of CotA and the pH value of the buffer determine to a great extent the net charge of the enzyme. The pH−charge profile can be calculated from the three-dimensional structure of the protein using the PROPKA 3.1 software package.[3,32] Using this approach, we determined a net charge for CotA of about −41 at pH 10.8 (see Figure S2 of the Supporting Information). PM2PV-*b*-PEO has a pH-independent charge of about +90. To form three-component micelles, the homopolymer PSS, which has a charge of about −188, was added to CotA solutions with a charge concentration 2, 4, or 6 times higher than that of CotA. To find the PMC for each of these cases, different concentrations of PM2PV-*b*-PEO were added to the CotA−PSS mixtures, and using DLS, the charge composition at which optimal micelle formation took place was determined.

Two- and three-component C3M solutions were prepared at their PMCs and stored at room temperature overnight before measurements. To monitor the salt stability of the C3Ms, a 4 M solution of NaCl was titrated to enzyme-containing micelles at their PMCs and observed by both DLS and FCS.

DLS. DLS was performed with an ALV instrument equipped with a DPSS laser operating at 660 nm. All measurements were performed at a scattering angle of 90° to determine the PMC, hydrodynamic radius, and polydispersity index (PDI). Multi-angle DLS was performed to determine the shape of the protein-containing C3Ms. The laser power used was 100 mW. The hydrodynamic radius R_h was calculated from the diffusion coefficient D,[46] obtained from the autocorrelation function by cumulant CONTIN analysis, and using the Stokes−Einstein equation, assuming spherical particles:

$$D = \frac{k_B T}{6\pi\eta R_h}$$

where k_B is the Boltzmann constant, T is the absolute temperature, and η is the viscosity of the solution.

FCS. FCS was performed using a Leica TCS SP8 X system equipped with a 63 × 1.2 NA water immersion objective and a supercontinuum laser. CotA labeled with Alexa Fluor 488 was excited by selecting the 488 nm laser line with a pulse frequency of 40 MHz. Fluorescence was collected through a size-adjustable pinhole, set at 1 Airy unit, and filtered using a 495−525 nm spectral filter using a hybrid detector coupled to a PicoHarp 300 TCSPC module (PicoQuant). FCS data were analyzed with software FFS data processor, version 2.3 (Scientific Software Technologies Software Centre, Belarus), using a two-component three-dimensional (3D) diffusion model including a triplet state.[33] Rhodamine 110, which has a diffusion coefficient of 4.3×10^{-10} m^2 s^{-1}, was used to determine the confocal structure parameter ($a = \omega_z/\omega_{xy}$, where ω_{xy} and ω_z are the equatorial and axial radii of the detection volume, respectively).

In FCS, fluorescent particles move in and out of the confocal volume, causing intensity fluctuations. These intensity fluctuations can be correlated with an autocorrelation function as follows:

$$G(t) = \frac{\langle I\rangle^2 + \langle \Delta I(t)\Delta I(t+\tau)\rangle}{\langle I\rangle^2}$$

where $G(t)$ is the normalized fluorescence fluctuation autocorrelation function, I is the fluorescence intensity, and $\Delta I(t)$ is the deviation of the average signal intensity at time t.

After excitation, intersystem crossing may occur, i.e., the transition of a fluorophore from the singlet state to the triplet state. Relaxation from the triplet state to the ground state can occur without emission of photons, and as a result, the fluorophore appears to be dark for a short interval. For autocorrelation analysis, this phenomenon needs to be considered because intersystem crossing to the triplet state may lead to an additional shoulder on the microsecond time scale.[34] For autocorrelation analysis, including the triplet state, the following equation applies:

$$G(\tau) = 1 + \frac{1}{\langle N\rangle}\frac{1 - T + T\,e^{-\tau/\tau_{trip}}}{(1-T)}\frac{1}{\left(1+\frac{\tau}{\tau_{dif}}\right)\sqrt{1+\left(\frac{\omega_{xy}}{w_z}\right)^2\frac{\tau}{\tau_{dif}}}}$$

where $\langle N\rangle$ is the average number of fluorescent particles in the confocal volume, τ_{trip} is the average time that a fluorophore resides in the triplet state, and τ_{dif} is the diffusion time of the fluorophore in the confocal volume. From the diffusion time, the diffusion coefficient D can be calculated using the following equation:

$$D = \frac{{\omega_{xy}}^2}{4\tau_{dif}}$$

Activity and Secondary Structure of the Encapsulated Enzyme. The activity of CotA-containing C3Ms was measured using the ABTS assay, and the protein secondary structure was determined using far-UV CD, as described above. During measurements, the temperature was kept to 25 °C. For each sample, the far-UV CD spectrum was recorded between 200 and 260 nm.

RESULTS AND DISCUSSION

pH Stability of CotA: Enzyme Activity and Secondary Structure. To encapsulate CotA in C3Ms using a positively charged diblock copolymer, a high pH of 10.8 was chosen to establish a sufficient negative charge on the enzyme and to eliminate the effect of the positively charged patch on its surface.

The activity of CotA as a function of the incubation time at different pH values is presented in Figure 2. It shows that CotA laccase activity does not depend upon the time of incubation and is an alkali-resistant enzyme. As described in the Introduction, the active site of CotA involves Cu ions; incubation of the enzyme at high pH results in an increase

https://dx.doi.org/10.1021/acs.langmuir.0c01073
Langmuir 2020, 36, 8494−8502

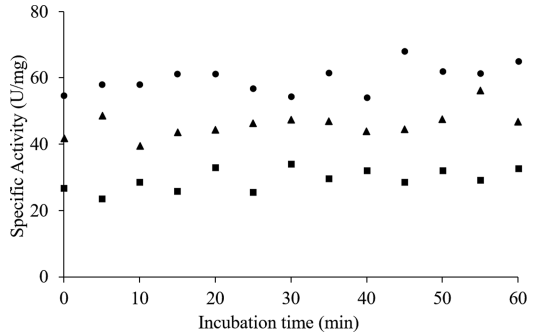

Figure 2. Specific activity of CotA measured at pH 4.4 after incubation of the enzyme at different pH values (●, pH 10.8; ▲, pH 9.0; and ■, pH 7.6) as a function of the incubation time at 25 °C.

of the redox potential of CotA, where T1 Cu in the enzyme will have a higher tendency to gain electrons from the substrate, speeding up the catalytic cycle.[35] The incubation at high pH may also increase the reduction rate of the oxidized trinuclear cluster, which then becomes faster available again for further reaction with O_2.[36,37]

The CD spectra presented in Figure 3 show that the secondary structure of CotA laccase is not significantly affected by incubation at high pH; the functional conformation of the enzyme is maintained, despite the deprotonation of amino acid residues at alkaline pH.

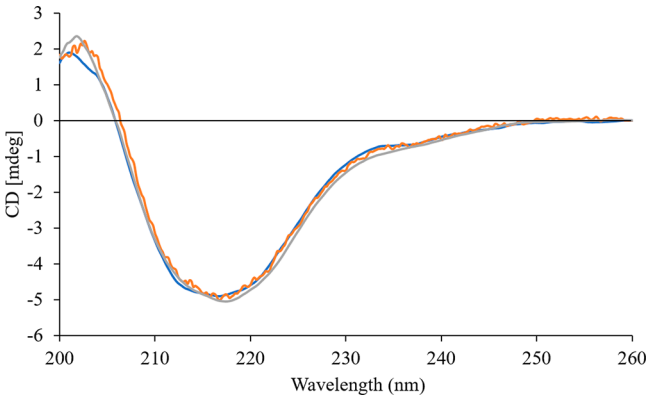

Figure 3. CD spectra of CotA measured after incubation for 1 h at different pH values measured at the pH of incubation (orange line, pH 10.8; gray line, pH 9.0; and blue line, pH 7.6).

Complex Coacervate Core Micelles: Two-Component Micelles. Two-component complex coacervate core micelles were obtained by mixing CotA with $PM2PV_{128}$-*b*-PEO_{477}. At neutral pH, CotA has a highly positive patch on its surface as a result of 10 lysines and 5 arginines that are located at the interface between domains 1, 2, and 3,[23] while the net charge of the CotA molecules is negative (−10). At low ionic strengths, this can lead to electrostatic protein−protein interactions. Adding the diblock copolymer PM2PV-*b*-PEO to the protein solution at neutral pH led to the formation of heterogeneous large aggregates and precipitation (data not shown). For the formation of C3Ms, it is therefore essential to decrease the charge anisotropy of the protein by neutralization of the lysine residues in the protein by increasing the pH.[13]

At pH 10.8, the formation of C3Ms consisting of CotA and PM2PV-*b*-PEO was successful. At this pH, the net charge on the protein amounts to −41. The charge composition of the system can be described by partition coefficient F^- according to the equation

$$F^- = \frac{n^-}{n^- + n^+}$$

where $n^- = c^-N^-$ and $n^+ = c^+N^+$, i.e., the total concentration of negative charges and the total concentration of positive charges on the two types of macromolecules, respectively, where c is their molar concentrations and N is the number of charged groups per molecule.

To determine the PMC, usually a solution with a constant amount of polyelectrolyte or charged biomolecule is mixed with increasing amounts of diblock copolymer. At the PMC, the concentration of micelles reaches a maximum, and using DLS, this can be detected as a maximum in light scattering intensity.[47] When F^- is far from the PMC, the interaction between the polyelectrolyte (biomolecule) and oppositely charged diblock would only produce a limited number of small soluble complexes, resulting in low light scattering intensities.[8,3]

DLS measurements on solutions with varying charge compositions (mixing ratios) show the highest intensity at F^- = 0.5 (Figure 4A), implying that the PMC corresponds to

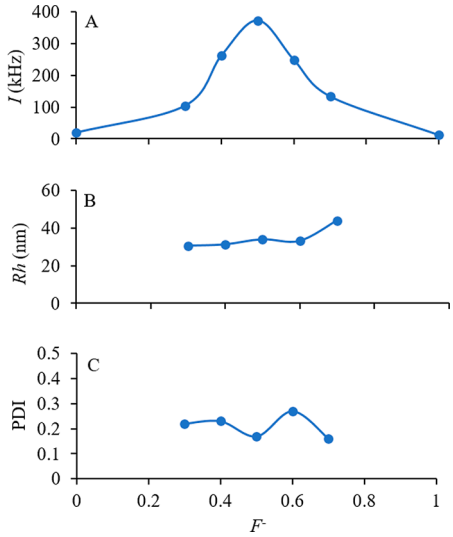

Figure 4. DLS results for mixtures of CotA and $PM2PV_{128}$-*b*-PEO_{477} as a function of the charge composition F^-: (A) scattering intensity (I), (B) hydrodynamic radius (R_h), and (C) PDI.

equal concentrations of positive and negative charges on the diblock and the protein. At the PMC, the scattering objects have a hydrodynamic radius of 34.0 ± 0.8 nm (Figure 4B). At the PMC, a minimum in the PDI is found (Figure 4C), indicating a narrow size distribution of the formed micelles.

The shape of the micelles can be determined using multi-angle DLS. At each detection angle, the decay rate Γ of the DLS correlation function is determined by means of cumulant fits. From Figure 5, it can be seen that Γ fitted with the first, second, and third cumulants as a function of the squared wave vector (q^2) gives three overlapping straight lines, showing that the C3Ms are spherical and monodisperse.[38] The slope of the lines equals the diffusion coefficient.

Activity measurements were performed for samples with various mixing ratios of CotA and diblock copolymer, where F^- = 0 is only polymer and F^- = 1 is only enzyme. Except for

https://dx.doi.org/10.1021/acs.langmuir.0c01073
Langmuir 2020, 36, 8494−8502

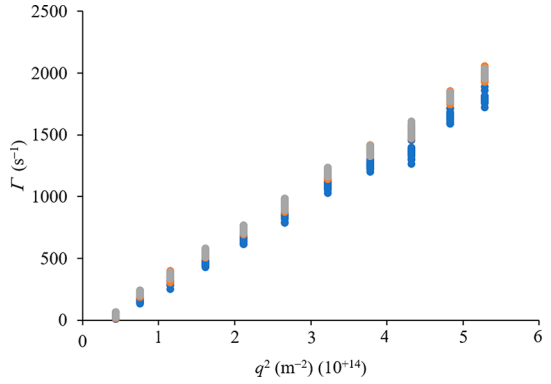

Figure 5. Multi-angle DLS results for two-component enzyme-containing C3Ms. Decay rate Γ (q) obtained from the DLS correlation curves by a first (blue), second (orange), and third (gray) cumulant fit.

F^- = 0, all samples had the same enzyme concentration. The activity of CotA was found to be constant (Figure 6) and similar to the activity of free enzyme incubated at pH 10.8 (Figure 2). It should be noted that the mixed samples were prepared at pH 10.8, but the ABTS test was carried out at pH 4.4. At this lower pH, CotA will be released from the micelles and then oxidize the substrate ABTS. Packing and subsequent release from the C3Ms apparently did not affect the activity of the enzyme. The CD results (Figure 7) confirmed that the secondary structure of the enzyme was maintained when the enzyme was encapsulated in C3Ms.

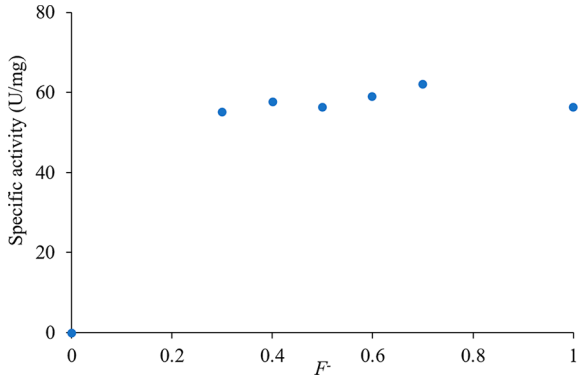

Figure 6. Specific activity of CotA measured after being encapsulated in different charge ratios with the diblock copolymer.

Complex Coacervate Core Micelles: Three-Component Micelles. To obtain three-component micelles, the negatively charged homopolymer PSS_{215} was added to mixtures of CotA and $PM2PV_{128}$-*b*-PEO_{477} with a charge concentration 2, 4, or 6 times higher than that of CotA. DLS measurements showed that for all PSS/CotA charge concentration ratios, a maximum in light scattering intensity was observed at an overall charge composition of F^- = 0.6 (Figure 8A), indicating that micelles are mostly formed at this mixing composition. The deviation of the PMC from 0.5 suggests that micelle formation is not only due to electrostatic interactions and counterion release but that other interactions also play a role, most likely hydrophobic interactions. CotA has several hydrophobic residues at its surface with different levels of exposure. The polyelectrolytes used in this study also have hydrophobic parts, i.e., the vinyl backbone of PM2PV-*b*-PEO

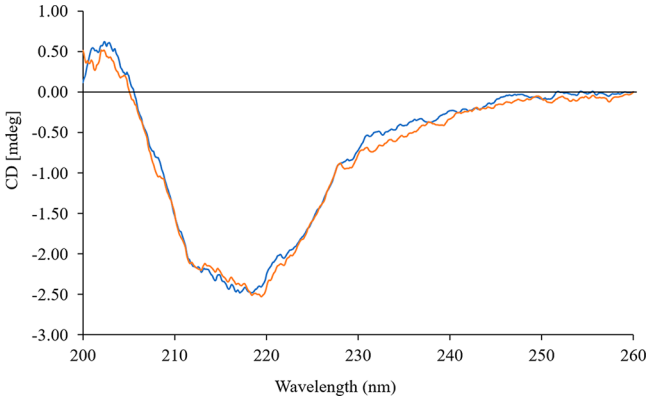

Figure 7. CD spectra of two-component enzyme-containing C3Ms (orange line) and the free enzyme (blue line).

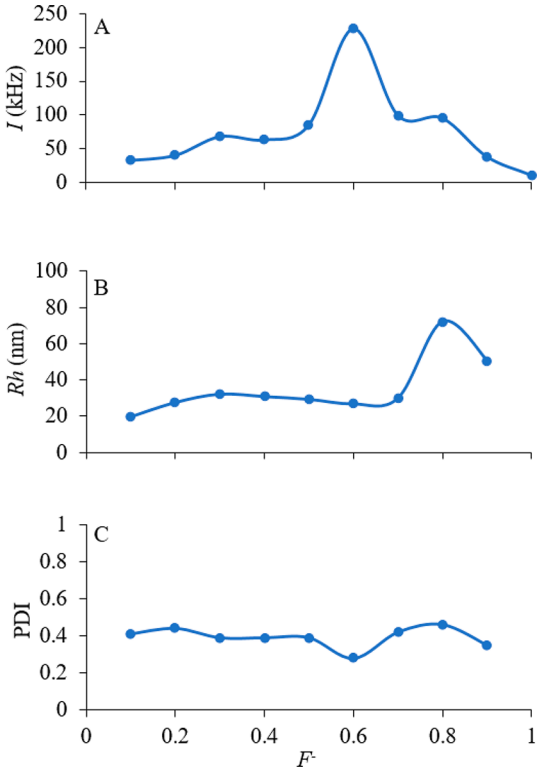

Figure 8. DLS results for three-component C3Ms (with a PSS/CotA charge ratio of 2:1) as a function of charge composition F^-: (A) scattering intensity (I), (B) hydrodynamic radius (R_h), and (C) PDI.

and the styrene group of PSS, and these could be involved in protein−polyelectrolyte interactions.[13] It seems that hydrophobic interactions are more important in the three-component micelles than in the two-component micelles (PMC at F^- = 0.5).

At the PMC of the three-component C3Ms, the lowest PDI was found compared to other mixing ratios (Figure 8C). The hydrodynamic radii of the three-component micelles are about 26.6 ± 0.5, 24.2 ± 0.2, and 23.6 ± 0.5 nm for 2, 4, and 6 times higher charge concentrations to CotA, respectively (Figure 8B). Similar results were obtained upon changing the mixing order of enzyme, homopolymer, and diblock copolymer (see Figures S4 and S5 of the Supporting Information). The addition of the homopolymer results in smaller micelles than the size of two-component C3Ms, which suggests that the

https://dx.doi.org/10.1021/acs.langmuir.0c01073
Langmuir 2020, 36, 8494−8502

amount of encapsulated enzyme molecules per micelle is less in the three-component C3Ms. As shown in Figure 9, multi-angle DLS results indicate that three-component C3Ms also have a spherical shape and are fairly monodisperse, similar to the two-component C3Ms.

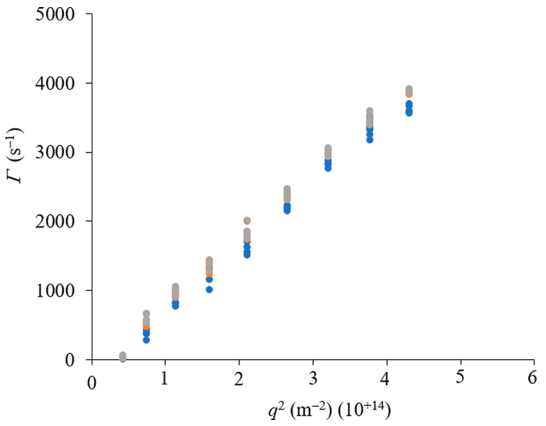

Figure 9. Multi-angle DLS results for three-component C3Ms with a PSS/CotA charge ratio of 2. Decay rate $\Gamma(q)$ obtained from the DLS correlation curves by a first (blue), second (orange), and third (gray) cumulant fit. Similar trend lines were also observed for the PSS/CotA charge ratios of 4 and 6.

FCS Analysis of Two- and Three-Component C3Ms. Native CotA is not fluorescent in the visible spectrum; therefore, the CotA S313C variant was used for labeling with the fluorescent dye Alexa Fluor 488 via a maleimide reaction and after purification (see Figure S3 of the Supporting Information), applied in FCS experiments.[39]

The two- and three-component C3Ms were prepared using labeled CotA at their PMCs obtained from the DLS measurements. FCS analysis allows for the discrimination between CotA free in solution (small particles) and incorporated into micelles (large particles) based on their different diffusion times. In addition, the enzyme-containing C3Ms are much brighter than the free enzyme molecules. The fluorescence intensity of the C3Ms is expected to be proportional to the number of encapsulated proteins.

The normalized autocorrelation curves in Figure 10 show a faster decay and, thus, a larger diffusion coefficient for the solution that contained only fluorescently labeled CotA than for the mixture of CotA and the diblock copolymer. In addition, the number of fluorescent particles detected in the confocal volume (N) was much higher for the solution without the diblock copolymer (87 versus 3 particles; data not shown), with a much lower fluorescence intensity. These results confirm the encapsulation of labeled CotA in C3Ms upon mixing with PM2PV-*b*-PEO and show that a large amount of CotA can be entrapped in the core of the two-component C3Ms.

The three-component systems also show a decrease in diffusion coefficients compared to the free CotA, while N decreased from 87 to 20, 19, and 30 for PSS charge concentrations of 2, 4, and 6 times that of CotA, respectively. The amplitude of the autocorrelation curve of the particles in the three-component systems is in between the amplitude of the free labeled CotA and that of the two-component C3Ms. These results show that CotA is also encapsulated in the three-component C3Ms, with a lower amount of encapsulated

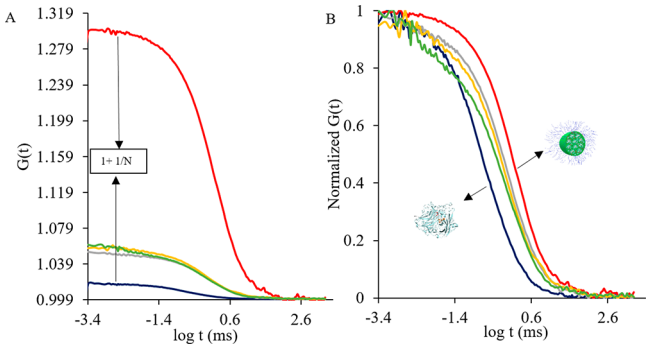

Figure 10. Autocorrelation curves obtained with FCS: (A) not normalized $G(t)$ and (B) normalized $G(t)$. Blue curves represent free labeled CotA, and red curves represent the two-component C3Ms. Gray, yellow, and green curves represent the three-component C3Ms made using 2-, 4-, and 6-fold charge excess of PSS over CotA, respectively. The total CotA concentration was identical in all samples.

enzyme molecules per micelle than in the two-component system.

Further analysis of the FCS results revealed that free labeled CotA has R_h of about 2.4 ± 0.2 nm. In the two-component system, about 84% of the enzyme was present in micelles, with a R_h of about 38 nm. The three-component C3Ms appeared smaller, having a size of about 24 nm, and here about 80% of the CotA is encapsulated in the core of micelles. Apparently, there is no significant difference in encapsulation efficiency among the three-component micelles made with different charge ratios of CotA and PSS. This is probably because, for the samples with different CotA/PSS ratios, the total CotA concentration was kept constant, while the concentration of the diblock copolymer PM2PV-*b*-PEO was increased with the concentration of PSS to keep F^- at −0.6 (the PMC). As a result, more micelles are formed but with a lower amount of CotA per micelle. The hydrodynamic radii found with FCS are similar to those obtained with DLS.

Stability of Two- and Three-Component C3Ms against Salt. FCS can provide information on the fractions of CotA encapsulated in C3Ms and free in solution, data that is not provided by DLS. We used both techniques to monitor the change in stability of the enzyme-containing C3Ms upon the addition of salt (NaCl). From the DLS results in Figure 11, it can be seen that, by stepwise adding salt to the two-component C3M system, the scattering intensity and the R_h of the micelles gradually decrease. These phenomena occur because, upon increasing the salt concentration, the electrostatic interactions become weaker and the entropy gain from counterion release becomes smaller, leading to a lower stability constant for C3M formation.[40] As a result, the micelles start to disintegrate.[41,48−51] The DLS data clearly show that the addition of the homopolymer improved the salt stability of the protein-containing C3Ms. The more PSS present in the system, the more resistant it is toward salt addition. We found that, in the limiting case of an infinite ratio PSS/CotA, i.e., for micelles consisting of only homopolymer PSS and diblock copolymer PM2VP-*b*-PEO, the system was still stable at 1 M NaCl (data not shown). This is in line with the observation of van der Gucht et al. that, for mixtures of the polyelectrolytes $PM2VP_{88}$ and PSS_{165}, the critical salt concentration, i.e., the salt concentration above which no coacervate phase is formed, amounts to about 2 M (KCl).[44] We assume the limit of the salt

https://dx.doi.org/10.1021/acs.langmuir.0c01073
Langmuir 2020, 36, 8494−8502

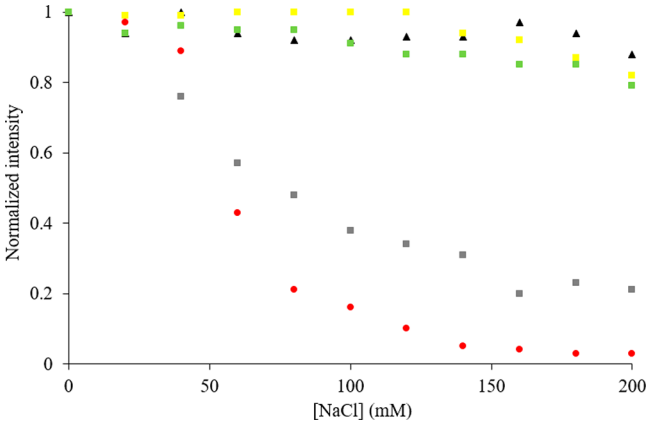

Figure 11. Normalized DLS scattering intensity for salt titration (NaCl) of C3M solutions. Circles (red) represent the two-component C3MS of CotA and the diblock copolymer. Triangles (black) represent micelles formed only by the homopolymer and the diblock copolymer. Squares represent three-component C3Ms made with 2 (gray), 4 (yellow), and 6 (green) time charge excess of PSS over CotA.

stability of the C3Ms with increasing the PSS content is also well above 1.5 M salt.

DLS data cannot provide changes in the number of CotA encapsulated in C3Ms upon increasing the ionic strength. Therefore, we used FCS as a read-out because this technique allows for distinguishing between the fraction of the free enzyme (fraction 1) and the fraction of the enzyme encapsulated in C3Ms in the confocal volume (fraction 2). With the addition of salt, fraction 2 decreased, corresponding to an increase in fraction 1. As shown in Figure 12, the total

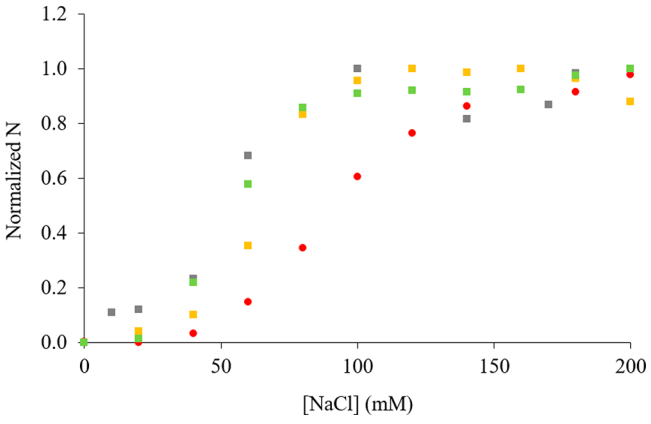

Figure 12. FCS analysis for salt titration of two- and three-component C3Ms: normalized number of particles *N* in the confocal volume. Circles (red) represent the two-component C3MS of CotA and the diblock copolymer. Squares represent three-component C3Ms made with 2 (gray), 4 (yellow), and 6 (green) time charge excess of PSS over CotA.

number of fluorescent particles detected in the confocal volume (*N*) also increased upon stepwise addition of salt, indicating the release of CotA as well. These results clearly show that CotA was released from the three-component C3Ms at a significantly lower salt concentration and over a narrower salt concentration range than from the two-component C3Ms. Evidently, the presence of PSS caused CotA to be expelled from the micelles upon the addition of salt, even though the DLS results showed that the micelles become more salt-resistant with the presence of PSS. Therefore, the addition of the homopolymer with the same charge sign as the enzyme is not an appropriate strategy for improving the stability of enzyme-containing C3Ms in a high salt environment.

An explanation for the FCS results is that the attraction between PM2PV-*b*-PEO and PSS is stronger than that between PM2PV-*b*-PEO and CotA, because PSS has a much higher charge density than CotA. Therefore, the homopolymer is preferably taken up in the micelles, and only a relatively small amount of negatively charged CotA contributes to the stoichiometry. When salt is added to the micellar solution, the electrostatic interactions decrease and especially the attraction between the protein and diblock copolymer becomes very weak. Moreover, the enzyme is a bulky molecule with only a few charges, and with the addition of small ions, it becomes entropically no longer favorable to incorporate the enzyme in the C3Ms.[42] As a result, the enzyme is expelled from the complex coacervate core and replaced by a homopolymer.[43]

Adding salt to C3M solutions also affects the micellar dynamics. With increasing the ionic strength, intermolecular exchange processes will be faster as well as rearrangements in the micellar core.[52,3] This facilitates the replacement of CotA by PSS.

CONCLUSION

Using DLS and FCS, we showed that, at high pH (10.8), the enzyme CotA can be encapsulated with the diblock copolymer PM2PV-*b*-PEO into complex coacervate core micelles. At neutral pH, micelle formation does not take place, most likely because of the low net negative charge of the enzyme and the presence of a positively charged patch on its surface. To improve the salt stability of the micelles, the negatively charged homopolymer PSS was added to create three-component C3Ms. The three-component C3Ms are smaller (hydrodynamic radius of 24 versus 32 nm for the two-component system), and FCS measurements showed that, per micelle, less CotA is encapsulated, although the fraction of enzyme that is encapsulated is still high (80 versus 84%). DLS measurements confirmed that the three-component C3Ms are indeed more salt-resistant than the two-component C3Ms. However, FCS analysis revealed that CotA is expelled from the three-component C3Ms already at relatively low salt concentrations.

From our results, it is clear that FCS experiments are vital to obtain insight into the composition and salt stability of the three-component C3Ms, because this technique enables discrimination between free CotA and encapsulated CotA. From these analyses, it can be concluded that adding a homopolymer with the same charge sign as the protein is not a good strategy to improve the salt stability of protein-containing C3Ms. We suggest that it is important to increase the charge density of the enzyme by the bioconjugation technique, and then enzyme-containing C3Ms become more salt-resistant.

ASSOCIATED CONTENT

Supporting Information

The Supporting Information is available free of charge at https://pubs.acs.org/doi/10.1021/acs.langmuir.0c01073.

^{1}H NMR of PM2PV$_{128}$-*b*-PEO$_{477}$ (Figure S1), charge of CotA as a function of pH calculated using the PROPKA 3.1 software package (Figure S2), SDS−PAGE analysis

https://dx.doi.org/10.1021/acs.langmuir.0c01073
Langmuir 2020, 36, 8494−8502

for CotA laccase (Figure S3), and effect of changing the mixing order (Figures S4 and S5) (PDF)

AUTHOR INFORMATION

Corresponding Author

Jan Willem Borst − *Laboratory of Biochemistry, Microspectroscopy Research Facility, Wageningen University and Research, 6708 WE Wageningen, Netherlands;* orcid.org/0000-0001-8176-9302; Email: janwillem.borst@wur.nl

Authors

Riahna Kembaren − *Physical Chemistry and Soft Matter and Laboratory of Biochemistry, Microspectroscopy Research Facility, Wageningen University and Research, 6708 WE Wageningen, the Netherlands*

Remco Fokkink − *Physical Chemistry and Soft Matter, Wageningen University and Research, 6708 WE Wageningen, the Netherlands*

Adrie H. Westphal − *Laboratory of Biochemistry, Microspectroscopy Research Facility, Wageningen University and Research, 6708 WE Wageningen, Netherlands*

Marleen Kamperman − *Zernike Institute for Advanced Research, University of Groningen, 9747 AG Groningen, the Netherlands;* orcid.org/0000-0002-0520-4534

J. Mieke Kleijn − *Physical Chemistry and Soft Matter, Wageningen University and Research, 6708 WE Wageningen, the Netherlands*

Complete contact information is available at: https://pubs.acs.org/10.1021/acs.langmuir.0c01073

Notes

The authors declare no competing financial interest.

ACKNOWLEDGMENTS

This work was supported by the VLAG Graduate School, Wageningen University and Research Center. The authors thank Prof. Willem van Berkel and Prof. Jasper van der Gucht for their valuable suggestions and discussions.

REFERENCES

(1) Agarwal, N. P.; Matthies, M.; Gur, F. N.; Osada, K.; Schmidt, T. L. Block Copolymer Micellization as a Protection Strategy for DNA Origami. *Angew. Chem., Int. Ed.* **2017**, *56*, 5460−5464.

(2) Itaka, K.; Kanayama, N.; Nishiyama, N.; Jang, W.-D.; Yamasaki, Y.; Nakamura, K.; Kawaguchi, H.; Kataoka, K. Supramolecular Nanocarrier of siRNA from PEG-based Block Catiomer Carrying Diamide Side Chain with Distinctive pK_a Directed to Enhance Intracellular Gene Silencing. *J. Am. Chem. Soc.* **2004**, *126*, 13612−13613.

(3) Nolles, A.; Westphal, A. H.; de Hoop, J. A.; Fokkink, R. G.; Kleijn, J. M.; van Berkel, W. J. H.; Borst, J. W. Encapsulation of GFP in Complex Coacervate Core Micelles. *Biomacromolecules* **2015**, *16*, 1542−1549.

(4) Mills, C. E.; Obermeyer, A.; Dong, X.; Walker, J.; Olsen, B. D. Complex Coacervate Core Micelles for the Dispersion and Stabilization of Organophosphate Hydrolase in Organic Solvents. *Langmuir* **2016**, *32*, 13367−13376.

(5) Voets, I. K.; de Keizer, A.; Cohen Stuart, M. A. Complex Coacervate Core Micelles. *Adv. Colloid Interface Sci.* **2009**, *147−148*, 300−318.

(6) Khullar, P.; Singh, V.; Mahal, A.; Kumar, H.; Kaur, G.; Bakshi, M. S. Block Copolymer Micelles as Nanoreactors for Self-assembled Morphologies of Gold Nanoparticles. *J. Phys. Chem. B* **2013**, *117* (10), 3028−3039.

(7) Bourouina, N.; Cohen Stuart, M. A.; Kleijn, J. M. Complex Coacervate Core Micelles as Diffusional Nanoprobes. *Soft Matter* **2014**, *10*, 320−331.

(8) van der Burgh, S.; Fokkink, R.; de Keizer, A.; Cohen Stuart, M. A. Complex Coacervation Core Micelles as Anti-Fouling Agents on Silica and Polystyrene Surfaces. *Colloids Surf., A* **2004**, *242*, 167−174.

(9) Mathot, F.; van Beijsterveldt, L.; Preat, V.; Brewster, M.; Arien, A. Intestinal Uptake and Biodistribution of Novel Polymeric Micelles after Oral Administration. *J. Controlled Release* **2006**, *111*, 47−55.

(10) Sant, V. P.; Smith, D.; Leroux, J.-C. Enhancement of Oral Bioavailability of Poorly Water-Soluble Drugs by Poly(Ethylene Glycol)-*block*-Poly(Alkyl Acrylate-*co*-Methacrylic Acid) Self-Assemblies. *J. Controlled Release* **2005**, *104*, 289−300.

(11) Kotz, J.; Kosmella, S.; Beitz, T. Self-assembled Polyelectrolyte Systems. *Prog. Polym. Sci.* **2001**, *26*, 1199−1232.

(12) Hofs, B.; Voets, I. K.; de Keizer, A.; Cohen Stuart, M. A. Comparison of Complex Coacervate Core Micelles from Two Diblock Copolymers or a Single Diblock Copolymer with a Polyelectrolyte. *Phys. Chem. Chem. Phys.* **2006**, *8*, 4242−4251.

(13) Cooper, C. L.; Dubin, P. L.; Kayitmazer, A. B.; Turksen, S. Polyelectrolyte-Protein Complexes. *Curr. Opin. Colloid Interface Sci.* **2005**, *10*, 52−78.

(14) Lindhoud, S.; de Vries, R.; Norde, W.; Cohen Stuart, M. A. Structure and Stability of Complex Coacervate Core Micelles with Lysozyme. *Biomacromolecules* **2007**, *8* (7), 2219−2227.

(15) Black, K. A.; Priftis, D.; Perry, S. L.; Yip, J.; Byun, W. Y.; Tirrell, M. Protein Encapsulation via Polypeptide Complex Coacervation. *ACS Macro Lett.* **2014**, *3* (10), 1088−1091.

(16) Blocher, W. C.; Perry, S. L. Complex Coacervate-Based Materials for Biomedicine. *WIREs Nanomed. Nanobiotechnol.* **2017**, *9* (4), e1442.

(17) Gapiński, J.; Szymański, J.; Wilk, A.; Kohlbrecher, J.; Patkowski, A.; Hołyst, R. Size and Shape of Micelles Studied by Means of SANS, PCS, and FCS. *Langmuir* **2010**, *26* (12), 9304−9314.

(18) Elson, E. L. Fluorescence Correlation Spectroscopy: Past, Present, Future. *Biophys. J.* **2011**, *101* (12), 2855−2870.

(19) Martins, L. O.; Soares, C. M.; Pereira, M. M.; Teixeira, M.; Costa, T.; Jones, G. H.; Henriques, A. O. Molecular and Biochemical Characterization of a Highly Stable Bacterial Laccase that Occurs as a Structural Component of the *Bacillus subtilis* Endospore Coat. *J. Biol. Chem.* **2002**, *277* (21), 18849−18859.

(20) Guzik, U.; Hupert-Kocurek, K.; Wojcieszynska, D. Immobilization as Strategy for Improving Enzyme Properties—Application to Oxidoreductases. *Molecules* **2014**, *19*, 8995−9018.

(21) Shraddha; Shekher, R.; Sehgal, R.; Kamthania, M.; Kumar, A. Laccase: Microbial Sources, Production, Purification, and Potential Biotechnological Applications. *Enzyme Res.* **2011**, *2011*, 1−11.

(22) Fernandes, A. T.; Lopes, C.; Martins, L. O.; Melo, E. P. Unfolding Pathway of CotA-Laccase and the Role of Copper on the Prevention of Refolding through Aggregation of the Unfolded State. *Biochem. Biophys. Res. Commun.* **2012**, *422* (3), 442−446.

(23) Enguita, F. J.; Martins, L. O.; Henriques, A. O.; Carrondo, M. A. Crystal Structure of a Bacterial Endospore Coat Component. A Laccase with Enhanced Thermostability Properties. *J. Biol. Chem.* **2003**, *278* (21), 19416−19425.

(24) Beneyton, T.; Beyl, Y.; Guschin, D. A.; Griffiths, A. D.; Taly, V.; Schuhmann, W. The Thermophilic CotA Laccase from *Bacillus subtilis*: Bioelectrocatalytic Evaluation of O_2 Reduction in the Direct and Mediated Electron Transfer Regime. *Electroanalysis* **2011**, *23* (8), 1781−1789.

(25) Liu, Z.; Xie, T.; Zhong, Q.; Wang, G. Crystal Structure of CotA Laccase Complexed with 2,2-azinobis-(3-ethylbenzothiazoline-6-sulfonate) at a Novel Binding Site. *Acta Crystallogr., Sect. F: Struct. Biol. Commun.* **2016**, *72* (4), 328−35.

(26) Pich, A.; Bhattacharya, S.; Adler, H.-J. P.; Wage, T.; Taubenberger, A.; Li, Z.; van Pee, K.-H.; Böhmer, U.; Bley, T. Composite Magnetic Particles as Carriers for Laccase from *Trametes versicolor*. *Macromol. Biosci.* **2006**, *6* (4), 301−310.

(27) Bryjak, J.; Kruczkiewicz, P.; Rekuc, A.; Peczynska-Czoch, W. Laccase Immobilization on Copolymer of Butyl Acrylate and Ethylene Glycol Dimethacrylate. *Biochem. Eng. J.* **2007**, *35*, 325−332.
(28) Christopher, L. P.; Yao, B.; Ji, Y. Lignin Biodegradation with Laccase-Mediator Systems. *Front. Energy Res.* **2014**, *2* (12), 1−13.
(29) Lindhoud, S.; Norde, W.; Cohen Stuart, M. A. Effect of Polyelectrolyte Complex Micelles and their Components on the Enzymatic Activity of Lipase. *Langmuir* **2010**, *26* (12), 9802−9808.
(30) Fulmer, G. R.; Miller, A. J. M.; Sherden, N. H.; Gottlieb, H. E.; Nudelman, A.; Stoltz, B. M.; Bercaw, J. E.; Goldberg, K. I. NMR Chemical Shifts of Trace Impurities: Common Laboratory Solvents, Organics, and Gases in Deuterated Solvents Relevant to the Organometallic Chemist. *Organometallics* **2010**, *29* (9), 2176−2179.
(31) Durao, P.; Chen, Z.; Fernandes, A. T.; Hildebrandt, P.; Murgida, D. H.; Todorovic, S.; Pereira, M. M.; Melo, E. P.; Martins, L. O. Copper Incorporation into Recombinant CotA Laccase from *Bacillus subtilis*: Characterization of Fully Copper Loaded Enzymes. *JBIC, J. Biol. Inorg. Chem.* **2008**, *13*, 183−193.
(32) Rostkowski, M.; Olsson, M. H. M.; Søndergaard, C. R.; Jensen, J. H. Graphical Analysis of pH-Dependent Properties of Proteins Predicted Using PROPKA. *BMC Struct. Biol.* **2011**, *11* (1), 6.
(33) Skakun, V. V.; Engel, R.; Digris, A. V.; Borst, J. W.; Visser, A. J. W. G. Global Analysis of Autocorrelation Functions and Photon Counting Distributions. *Front. Biosci., Elite Ed.* **2011**, *E3* (2), 489−505.
(34) Skakun, V. V.; Hink, M. A.; Digris, A. V.; Engel, R.; Novikov, E. G.; Apanasovich, V. V.; Visser, A. J. W. G. Global Analysis of Fluorescence Fluctuation Data. *Eur. Biophys. J.* **2005**, *34* (4), 323−334.
(35) Singh, G.; Bhalla, A.; Kaur, P.; Capalash, N.; Sharma, P. Laccase from Prokaryotes: A New Source for an Old Enzyme. *Rev. Environ. Sci. Bio/Technol.* **2011**, *10*, 309−326.
(36) Solomon, E. I.; Chen, P.; Metz, M.; Lee, S.-K.; Palmer, A. E. Oxygen Binding, Activation, and Reduction to Water by Copper Proteins. *Angew. Chem., Int. Ed.* **2001**, *40* (24), 4570−4590.
(37) Solomon, E. I.; Augustine, A. J.; Yoon, J. O_2 Reduction to H_2O by the Multicopper Oxidases. *Dalton Trans.* **2008**, *30*, 3921−3932.
(38) Harada, A.; Kataoka, K. Novel Polyion Complex Micelles Entrapping Enzyme Molecules in the Core. 2. Characterization of the Micelles Prepared at Nonstoichiometric Mixing Ratios. *Langmuir* **1999**, *15*, 4208−4212.
(39) Toseland, C. P. Fluorescent Labeling and Modification of Proteins. *J. Chem. Biol.* **2013**, *6* (3), 85−95.
(40) Spruijt, E.; Westphal, A. H.; Borst, J. W.; Cohen Stuart, M. A.; van der Gucht, J. Binodal Compositions of Polyelectrolyte Complexes. *Macromolecules* **2010**, *43*, 6476−6484.
(41) van der Kooij, H. M.; Spruijt, E.; Voets, I. K.; Fokkink, R.; Cohen Stuart, M. A.; van der Gucht, J. On the Stability and Morphology of Complex Coacervate Core Micelles: From Spherical to Wormlike Micelles. *Langmuir* **2012**, *28*, 14180−14191.
(42) Lindhoud, S.; Claessens, M. M. A. E. Accumulation of Small Protein Molecules in a Macroscopic Complex Coacervate. *Soft Matter* **2016**, *12*, 408−413.
(43) Obermeyer, A. C.; Mills, C. E.; Dong, X.-H.; Flores, R. J.; Olsen, B. D. Complex Coacervation of Supercharged Proteins with Polyelectrolytes. *Soft Matter* **2016**, *12*, 3570−3581.
(44) van der Gucht, J.; Spruijt, E.; Lemmers, M.; Cohen Stuart, M. A. Polyelectrolyte Complexes: Bulk Phases and Colloidal Systems. *J. Colloid Interface Sci.* **2011**, *361*, 407−422.
(45) Nolles, A.; Westphal, A. H.; Kleijn, J. M.; van Berkel, W. J. H.; Borst, J. W. Colorful Packages: Encapsulation of Fluorescent Proteins in Complex Coacervate Core Micelles. *Int. J. Mol. Sci.* **2017**, *18* (7), 1557−1576.
(46) Stetefeld, J.; McKenna, S. A.; Patel, T. R. Dynamic Light Scattering: A Practical Guide and Applications in Biomedical Sciences. *Biophys. Rev.* **2016**, *8*, 409−427.
(47) van der Burgh, S.; de Keizer, A.; Cohen Stuart, M. A. Complex Coacervation Core Micelles. Colloidal stability and Aggregation Mechanism. *Langmuir* **2004**, *20*, 1073−1084.
(48) Lindhoud, S.; de Vries, R.; Schweins, R.; Cohen Stuart, M. A.; Norde, W. Salt-Induced Release of Lipase from Polyelectrolyte Complex Micelles. *Soft Matter* **2009**, *5* (1), 242−250.
(49) Lindhoud, S.; Voorhaar, L.; de Vries, R.; Schweins, R.; Cohen Stuart, M. A.; Norde, W. Salt-Induced Disintegration of Lysozyme-Containing Polyelectrolyte Complex Micelles. *Langmuir* **2009**, *25* (19), 11425−30.
(50) Wang, J.; de Keizer, A.; Fokkink, R.; Yan, Y.; Cohen Stuart, M. A.; van der Gucht, J. Complex Coacervate Core Micelles from Iron-Based Coordination Polymers. *J. Phys. Chem. B* **2010**, *114*, 8313−8319.
(51) Yan, Y.; de Keizer, A.; Cohen Stuart, M. A.; Drechsler, M.; Besseling, N. A. M. Stability of Complex Coacervate Core Micelles containing Metal Coordination Polymer. *J. Phys. Chem. B* **2008**, *112* (35), 10908−10914.
(52) Nolles, A.; Hooiveld, E.; Westphal, A. H.; van Berkel, W. J. H.; Kleijn, J. M.; Borst, J. W. FRET Reveals the Formation and Exchange Dynamics of Protein-Containing Complex Coacervate Core Micelles. *Langmuir* **2018**, *34*, 12083−12092.

https://dx.doi.org/10.1021/acs.langmuir.0c01073
Langmuir 2020, 36, 8494−8502